

Mind the Gap: Promoting Missing Modality Brain Tumor Segmentation with Alignment

Tianyi Liu
School of Robotics
Xi'an Jiaotong-Liverpool University
Suzhou, China
Tianyi.Liu2203@student.xjtlu.edu.cn

Zhaorui Tan
School of Advanced Technology
Xi'an Jiaotong-Liverpool University
Suzhou, China
Zhaorui.Tan21@student.xjtlu.edu.cn

Haochuan Jiang
School of Robotics
Xi'an Jiaotong-Liverpool University
Suzhou, China
h.jiang@xjtlu.edu.cn

Xi Yang
School of Advanced Technology
Xi'an Jiaotong-Liverpool University
Suzhou, China
xi.yang01@xjtlu.edu.cn

Kaizhu Huang
Data Science Research Center
Duke Kunshan University
Suzhou, China
kaizhu.huang@dukekunshan.edu.cn

Abstract—Brain tumor segmentation is often based on multiple magnetic resonance imaging (MRI). However, in clinical practice, certain modalities of MRI may be missing, which presents an even more difficult scenario. To cope with this challenge, knowledge distillation has emerged as one promising strategy. However, recent efforts typically overlook the modality gaps and thus fail to learn invariant feature representations across different modalities. Such drawback consequently leads to limited performance for both teachers and students. To ameliorate these problems, in this paper, we propose a novel paradigm that aligns latent features of involved modalities to a well-defined distribution anchor. As a major contribution, we prove that our novel training paradigm ensures a tight evidence lower bound, thus theoretically certifying its effectiveness. Extensive experiments on different backbones validate that the proposed paradigm can enable invariant feature representations and produce a teacher with narrowed modality gaps. This further offers superior guidance for missing modality students, achieving an average improvement of 1.75 on dice score.

Index Terms—Alignment, Brain Tumor Segmentation, Knowledge Distillation, Missing Modality

I. INTRODUCTION

Malignant brain tumors severely threaten people's lives. Accurate brain tumor segmentation is crucial for treatment planning [1]. Multiple Magnetic Resonance Imaging (MRI), such as Fluid Attenuation Inversion Recovery (Flair), contrast-enhanced T1-weighted (T1ce), T1-weighted (T1) and T2-weighted (T2), are common tools to segment brain tumors [2]. Since different modalities complement each other in understanding physical structure and physiopathology, combining them may naturally improve tumor segmentation [3]–[6].

The work was partially supported by the following: National Natural Science Foundation of China under No.92370119, No. 62206225, and No. 62376113; Jiangsu Science and Technology Program (Natural Science Foundation of Jiangsu Province) under No. BE2020006-4; Natural Science Foundation of the Jiangsu Higher Education Institutions of China under No. 22KJB520039; XJTLU Research Development Funding 20-02-60. Computational resources used in this research are provided by the School of Robotics, XJTLU Entrepreneur College (Taicang), Xi'an Jiaotong-Liverpool University.

However, due to difficulties such as data corruption and scanning protocol variations, in real clinical practice, certain modalities may often be missing [7]–[10]. Therefore, designing a generalized multi-modal approach to overcome difficulties brought by missing modalities is critical for practical clinical applications.

To address this challenge, knowledge distillation (KD) has emerged as one promising solution. Recent efforts in KD [1], [11]–[13] initially train a *teacher* with complete modalities that will then be used to supervise *students* to access missing modalities. To distill knowledge from *teachers*, KD-Net [12] employs the Kullback-Leibler (KL) loss to minimize the latent space divergence between *teachers* and *students*; PMKL [1] is later designed to enhance KD-Net by incorporating contrastive loss. Besides, ProtoKD [13] engages a prototype knowledge distillation loss to encourage simultaneous intra-class concentration and inter-class divergence. Moreover, Style matching U-Net addresses this problem by disentangling content and style components in the latent space [11].

While the above-mentioned wisdom enhances the segmentation capabilities of *students*, their effectiveness is limited by their *teachers* which remain sub-optimal and insufficiently explored. Concretely, in these methods, *teachers* simply treat different modalities as distinct channels and typically ignore the modality gaps. However, given that these MRI are captured by different imaging principles, modality gaps unfortunately exist as always (see Figure 1 (a)). As such, the *teachers* may fail to learn invariant features, which further prevents the model from learning shared representations across different modalities and consequently degrades the prediction performance.

Illuminated from alignment approaches in narrowing domain gaps in classification tasks [14]–[16], in this paper, we investigate whether alignment can also be used to reduce modality gaps for brain tumor segmentation tasks. To this end, we propose a novel **alignment paradigm** where *teachers*

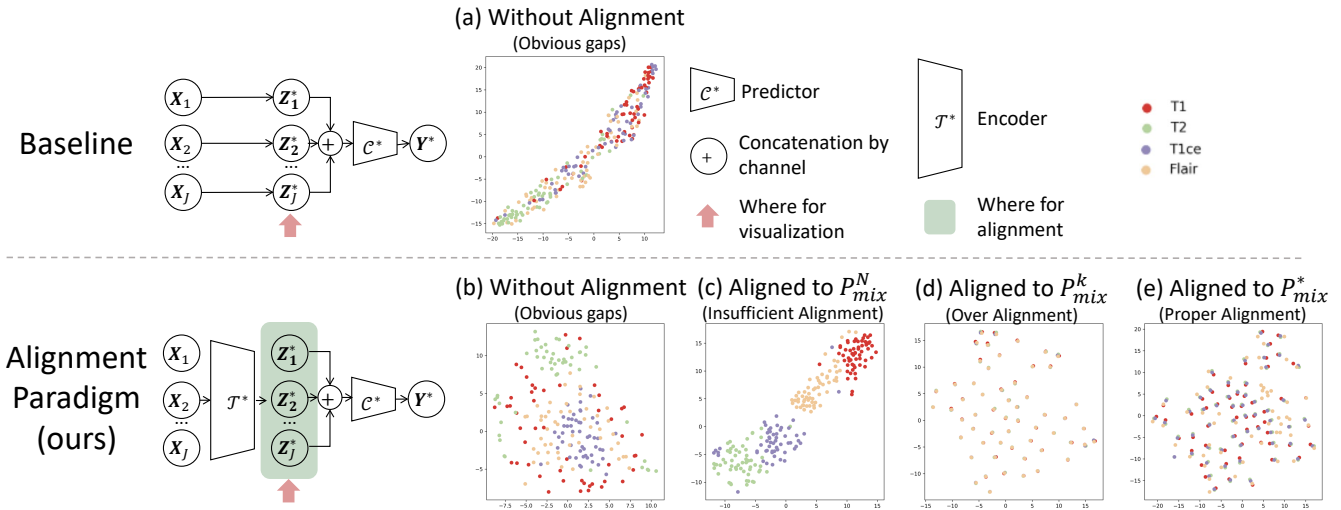


Fig. 1. Comparison results of T-SNE maps for *teachers*' latent features that are trained using different paradigms, whose structures are exhibited as diagrams. Data samples from each modality are assigned with a distinct color. For our paradigm, the latent space of each model is aligned to different empirical forms of P_{mix} : P_{mix}^N , P_{mix}^k and P_{mix}^* which will be discussed in Sec. III-B.

can indeed provide enhanced guidance to *student* by latent space alignment. Specifically, latent features of modalities are initially placed in the same space by employing an encoder. Inspired by VAE [17] and HeMIS [18], latent features of modalities are aligned to a pre-defined latent distribution as the anchor (termed as P_{mix}). It is worth noting that based on a series of theoretical analyses, we validate several possible empirical forms for P_{mix} . By analyzing the empirical evidence and the T-SNE [19] visualizations displayed in Figure 1, we reveal that the best P_{mix} is obtained by the weighted combination of each modality. As shown in Figures 1 (c) and (d), other options of P_{mix} 's yield inferior results. Furthermore, with the best P_{mix} , the proposed alignment paradigm fosters the learning of modality-invariant features by reducing modality gaps, producing a significant improvement on different modalities and different backbones. The major contributions of the paper are summarized as follows:

- We invent a novel alignment paradigm including a latent space distribution P_{mix} as the aligning anchor to learn cross-modality invariance.
- We provide theoretical support for the proposed alignment, showing that individually aligning each modality to the best P_{mix} certifies tighter Evidence Lower Bound than mapping all modalities as a whole to the P_{mix} .
- With extensive experiments, we verify the superiority of the proposed paradigm in promoting the brain tumor segmentation performance of both the *teacher* and the *students* in the latest state-of-the-art backbones.

II. THEORETICAL MOTIVATIONS

Notations. Considering J modalities of medical images with paired observations and targets $\{\mathbf{X}_j\}_{j=1}^J$ and \mathbf{Y} . Note for medical modalities, \mathbf{Y} remains static for all modalities. For the *teacher* of medical segmentation with missing modalities,

the encoders are denoted as $\mathcal{T} : \mathcal{T}(\mathbf{X}_j) \rightarrow \mathbf{Z}_j^*$ where \mathbf{Z}_j^* represents the produced latent features. Simultaneously, a predictor \mathcal{C} that predicts segmentation masks from $\{\mathbf{Z}_j^*\}_{j=1}^J$ as $\mathcal{C}^* : \mathcal{C}^*(\{\mathbf{Z}_j^*\}_{j=1}^J) \rightarrow \mathbf{Y}$. Correspondingly, we denote the possible downstream model for the j^{th} target modality as $\mathcal{S}_j : \mathcal{S}_j(\mathbf{X}_j) \rightarrow \mathbf{Z}_j$ of each modalities with their predictor $\mathcal{C}_j : \mathcal{C}_j(\mathbf{Z}_j) \rightarrow \mathbf{Y}$. Let $P(\cdot)$, $D_{KL}(\cdot||\cdot)$, $H_c(\cdot, \cdot)$, $I(\cdot; \cdot)$ denote the probability of a random variable from the distribution, KL divergence, cross-entropy, and mutual information, respectively.

Previous methods. The original objective used in [1], [11]–[13] of training *teacher* can be treated as using a fixed linear \mathcal{T} . Thus its objective is:

$$\max_{\mathcal{C}^*} \sum_{j=1}^J \mathbb{E}_{\mathbf{Z}_j^* \sim P(\mathbf{Z}_j^*)} [\ln P(\mathbf{Y} | \mathcal{C}^*(\mathbf{Z}_j^*))]. \quad (1)$$

In the scope of information theory, it can be altered as:

$$\min_{\mathcal{C}^*} \sum_{j=1}^J H_c(P(\mathcal{C}^*(\mathbf{Z}_j^*)), P(\mathbf{Y})). \quad (2)$$

Meanwhile, for \mathcal{S}_j that leverages knowledge from \mathcal{T} , its objective is:

$$\max_{\mathcal{S}_j, \mathcal{C}_j} \mathbb{E}_{\mathbf{Z}_j \sim P(\mathbf{Z}_j)} [\ln P(\mathbf{Y} | \mathcal{C}_j(\mathbf{Z}_j))] - D_{KL}(P(\mathbf{Z}_j) || P(\mathbf{Z}_j^*)). \quad (3)$$

In practice, the modality which \mathcal{S}_j aims to is unknown for \mathcal{T} . Thus, we expect the sum of risks for all possible *students* (shown in Eq. (3)) to be minimized:

$$\begin{aligned} & \max_{\mathcal{S}_j, \mathcal{C}_j} \sum_{j=1}^J [\mathbb{E}_{\mathbf{Z}_j \sim P(\mathbf{Z}_j)} [\ln P(\mathbf{Y} | \mathcal{C}_j(\mathbf{Z}_j))] - D_{KL}(P(\mathbf{Z}_j) || P(\mathbf{Z}_j^*))] \\ & = \min_{\{\mathcal{S}_j\}_{j=1}^J, \{\mathcal{C}_j\}_{j=1}^J} \sum_{j=1}^J [D_{KL}(P(\mathbf{Z}_j) || P(\mathbf{Z}_j^*)) \\ & \quad + H_c(P(\mathcal{C}_j(\mathbf{Z}_j)), P(\mathbf{Y}))]. \end{aligned} \quad (4)$$

Figure 1(a) illustrates that multi-modal medical images often exhibit incomplete space coverage and significant modality gaps, which can degrade the performance of *teachers*. In contrast, our experiments validate that the aligned latent space produced by our approach improves the generalization ability of the medical *teacher*, then benefiting downstream *students*.

Our alignment paradigm To alleviate the modality gaps, our alignment paradigm aligns all modal latent features to a pre-defined distribution P_{mix}^k , as shown in Figure 1(b) with P_{mix}^k and P_{mix}^* column. This part provides more details about our approach. Different from previous studies [1], [11]–[13], we further define a continuous distribution P_{mix} as the targeted latent space distribution of \mathbf{Z}^* for the *teacher*.

Proposition 1. *For training a multi-modal teacher model, it is assumed that $\mathbf{Z}_i \perp\!\!\!\perp \mathbf{Z}_j$ where $i, j \in \{1, \dots, J\}, i \neq j$. In this scenario, there exists a probability distribution P_{mix} that can be used as an anchor distribution to align the latent variables \mathbf{Z}^* , while preserving sufficient information for accurate prediction of the segmentation labels \mathbf{Y} .*

Proof. The modality-independent assumption is derived from the fact that each modality is independent of each other. If P_{mix} preserves sufficient information for accurate prediction of the segmentation labels \mathbf{Y} , based on the joint and marginal mutual information, we have

$$\sum_{j=1}^J I(P_{mix}(\mathbf{Z}_j^*); P(\mathbf{Z}_j^*)) \leq I(P_{mix}(\mathbf{Z}^*); P(\mathbf{Z}^*)). \quad (5)$$

Eq. (5) shows that individually mapping each modality \mathbf{Z}_j^* to P_{mix} is a lower bound of mapping all modalities together to P_{mix} . \square

Proposition 1 is **single-letterization** that simplifies the optimization problem over a large-dimensional (i.e., multi-letter) problem. Therefore, we individually align the representations of each modality to the anchor P_{mix} , rather than the whole distribution of all representations from all modalities:

$$\begin{aligned} & \sum_{j=1}^J \mathbb{E}_{\mathbf{Z}_j^* \sim P(\mathbf{Z}_j^*)} [\ln P(\mathbf{Y} | \mathcal{C}^*(\mathbf{Z}_j^*)) - D_{\text{KL}}(P(\mathbf{Z}_j^*) \| P_{mix})] \\ & \leq \mathbb{E}_{\mathbf{Z}^* \sim P(\mathbf{Z}^*)} [\ln P(\mathbf{Y} | \mathcal{C}^*(\mathbf{Z}^*)) - D_{\text{KL}}(P(\mathbf{Z}^*) \| P_{mix})]. \end{aligned} \quad (6)$$

The former is termed Evidence Lower Bound (ELBO) [17], which is tighter than the latter. Thus, minimizing the gap between all modalities and P_{mix} , the alternative objective for *teacher* is further derived as:

$$\min \sum_{j=1}^J [D_{\text{KL}}(P(\mathbf{Z}_j^*) \| P_{mix}) + H_c(P(\mathcal{C}^*(\mathbf{Z}_j^*)); P(\mathbf{Y}))]. \quad (7)$$

As shown in Eq. (7), the essential point is to find a feasible P_{mix} that anchors all latent features in the space while preserving the prediction ability from the latent features to targets for all *students*.

Possible approximations of P_{mix} . It is intractable to obtain the ideal P_{mix} in practice. Therefore, different pre-defined P_{mix} approximations are made. Similar to VAE, a possible

assumption is that P_{mix} is a fixed distribution such as standard normal distribution: $P_{mix}^N \triangleq \mathcal{N}(0, 1)$. However, P_{mix}^N may not certify Proposition 1, may yielding sub-optimal results. Thus, we propose P_{mix} which is one of $\{P(\mathbf{Z}_j^*)\}_{j=1}^J$ (i.e., $P_{mix}^k \triangleq P(\mathbf{Z}_{j=k}^*)$ where $k \in \{1, \dots, J\}$) or which is a weighted mixture of them (i.e., $P_{mix}^* \triangleq \sum_{j=1}^J w_j P(\mathbf{Z}_j)$) where w_j is the associated weight of each modality. P_{mix}^k and P_{mix}^* naturally preserve Proposition 1 through the prediction. Testing the effectiveness of the different P_{mix} , we find that a tractable approximation P_{mix}^* will produce approximately the best results.

III. METHODOLOGY

A. Proposed alignment paradigm

The overall alignment paradigm consists of training *teachers* and *students*. The structure diagram of the *teacher* is exhibited in the bottom left part of Figure 1. For training the *teacher*, each modality is initially encoded into the same latent space and then individually aligned to the pre-defined anchor P_{mix} as shown in Eq. (5). Finally, following the previous baselines, a 3D U-Net is used as the predictor (\mathcal{C}^*) for segmentation based on the aligned latent features.

Then the enhanced prior knowledge obtained by the *teachers* are leveraged to students by implanting to different backbones (see Sec. IV-A). We train *students* by distilling knowledge from the trained *teachers* in the missing modality scenario [1], [11]–[13]. The loss to be optimized is: $L^S = L_{seg}^S + L^T$, where L_{seg}^S represents the segmentation loss guided by ground truth labels, and L^T denotes the loss that receives supervision from the *teacher* used in the previous works.

B. Alignment with various P_{mix}

This alignment towards P_{mix} standardizes data distributions from diverse sources into a consistent distribution, facilitating the learning of unique features across modalities. Specifically, we provide details of the alignment to various empirical forms of P_{mix} (which are denoted as P_{mix}^k , P_{mix}^* , and P_{mix}^N).

Aligning to P_{mix}^k . The k^{th} modality that has the most feature invariant representation is a reasonable choice for P_{mix} (see more details in Sec. IV-C), i.e., $P_{mix}^k \triangleq P(\mathbf{Z}_{j=k}^*)$. The alignment of other modalities to the chosen optimal modality is facilitated through Mean Squared Error (MSE). Here we minimize: $\mathbb{E}[\|\mathbf{Z}_j^* - \mathbf{Z}_k^*\|^2]$ for each paired sample.

Aligning to P_{mix}^* . In the quest to derive a more conducive latent space for integrating all modalities, we have advanced an innovative methodology termed Adaptive Alignment. This approach will transcend the basic alignment method that confines the latent space to a specific modality. Adaptive Alignment operates under the presumption that an optimal latent space for a prior modality can serve as a foundational anchor. Then we have: $\sum_{j=1}^J w_j \|\mathbf{Z}_j^* - \mathbf{Z}_k^*\|^2$, where w_j are learnable weights. Note that the *teacher* is not frozen during training, with the purpose to enable the *teacher* find the adaptive latent space.

Aligning to P_{mix}^N . Since P_{mix}^k is the selected form $P(\mathbf{Z}_j^*)_1^J$ and P_{mix}^* is a weighted mixture of $P(\mathbf{Z}_j^*)_1^J$'s, the relationship

TABLE I

COMPARISON OF SEGMENTATION RESULTS IN EACH CLASS AND AVERAGE DICE SCORES WITH DIFFERENT ANCHOR P_{mix} .S. FOR EACH MODALITY, RESULTS ARE COMPARED TO A MODEL THAT ONLY USES UNIMODAL AND THE ORIGINAL BACKBONE MODELS. IMP.: IMPROVEMENT OF P_{mix}^* COMPARE TO ORIGINAL METHOD. AVERAGE IMP. IS THE AVERAGE IMPROVEMENT OF ALL THE IMP. COLUMN. THE BEST AVERAGE RESULTS OF EACH BACKBONE IF ALL SETTINGS ARE HIGHLIGHTED.

Method	Original Method				without Alignment				with P_{mix}^N				with P_{mix}^k				with P_{mix}^* Average Imp.: 1.75				Modality	
	WT	TC	EC	Avg.	WT	TC	EC	Avg.	WT	TC	EC	Avg.	WT	TC	EC	Avg.	WT	TC	EC	Avg.		Imp.
Unimodal	72.96	65.59	37.77	58.77	72.07	66.22	40.13	59.47	74.21	67.63	43.24	61.69	74.06	64.21	41.78	60.02	71.49	65.18	43.25	59.97	2.25	T1
KD-Net	79.62	59.83	33.69	57.72	80.50	66.99	48.02	65.17	83.23	69.64	43.18	65.35	83.22	70.72	44.72	66.22	84.26	71.30	47.04	67.53	5.48	
PMKL	73.31	64.26	41.37	58.98	75.50	65.98	40.09	60.53	75.60	65.59	43.31	61.50	75.06	66.80	41.43	61.10	72.04	68.39	47.66	62.70	3.97	
ProtoKD	74.46	67.34	47.41	63.07	73.64	65.05	43.04	60.57	72.95	65.52	42.92	60.47	75.60	66.95	43.18	61.91	73.98	67.36	42.11	61.15	-2.55	
SMU-Net	74.33	65.52	40.22	60.02	75.24	68.52	43.03	62.26	75.10	66.41	42.78	61.43	75.15	67.25	41.71	61.37	75.02	67.78	43.30	62.03	2.01	
Unimodal	82.65	66.76	45.23	64.91	80.50	66.99	48.02	65.17	83.23	69.64	43.18	65.35	83.22	70.72	44.72	66.22	84.26	71.30	47.04	67.53	5.48	T2
KD-Net	85.74	66.79	33.63	62.05	82.68	67.14	44.82	64.88	80.46	69.06	48.38	65.97	82.47	69.56	45.78	65.94	83.77	69.91	45.17	66.28	0.94	
PMKL	81.00	67.92	47.09	65.34	81.82	70.21	48.78	66.94	83.82	69.54	45.03	66.13	83.18	67.96	47.71	66.28	83.01	70.26	47.29	66.85	1.03	
ProtoKD	81.83	68.29	47.35	65.82	81.82	70.21	48.78	66.94	83.82	69.54	45.03	66.13	83.18	67.96	47.71	66.28	83.01	70.26	47.29	66.85	1.03	
SMU-Net	85.57	70.61	47.33	67.84	84.69	70.34	46.94	67.32	84.88	69.96	45.08	66.64	85.09	69.50	44.85	66.48	84.45	69.82	47.09	67.12	-0.62	
Unimodal	71.41	73.30	76.36	73.69	72.14	80.75	77.61	76.83	72.49	79.30	74.46	75.42	76.73	81.64	75.56	77.98	76.62	80.15	81.29	79.36	2.62	T1ce
KD-Net	78.87	80.83	70.52	76.74	74.00	78.64	72.71	77.31	73.89	80.86	77.48	77.41	77.46	80.71	75.40	77.86	75.97	80.35	76.44	77.58	3.26	
PMKL	70.50	76.92	75.54	74.32	74.00	78.64	72.71	77.31	73.89	80.86	77.48	77.41	77.46	80.71	75.40	77.86	75.97	80.35	76.44	77.58	3.26	
ProtoKD	74.67	81.48	76.01	77.39	75.16	80.47	76.74	77.45	76.82	80.85	77.43	77.70	75.98	79.41	76.99	77.46	74.91	81.47	76.99	77.91	0.52	
SMU-Net	75.33	79.41	76.22	76.99	76.65	80.08	76.01	77.58	75.68	79.86	74.92	76.06	78.63	74.85	76.51	76.66	75.83	80.13	75.57	77.18	0.09	
Unimodal	81.91	63.57	40.74	62.07	84.97	63.16	41.44	63.19	84.84	64.67	44.15	64.56	85.46	66.77	43.99	65.41	84.96	66.58	42.16	64.57	2.56	Flair
KD-Net	88.28	64.37	33.39	62.01	84.97	63.16	41.44	63.19	84.84	64.67	44.15	64.56	85.46	66.77	43.99	65.41	84.96	66.58	42.16	64.57	2.56	
PMKL	84.11	62.21	41.35	62.56	84.74	67.07	43.42	65.07	84.09	66.78	42.13	64.33	83.84	68.89	41.41	64.71	85.70	68.44	43.57	65.90	3.06	
ProtoKD	84.64	65.56	42.30	64.17	84.59	67.70	40.91	64.39	84.62	64.32	37.76	62.23	84.23	67.73	41.45	64.47	85.62	68.71	41.38	65.23	1.34	
SMU-Net	85.74	62.89	38.12	62.25	85.70	63.50	39.43	62.88	85.99	65.74	40.55	64.09	86.78	63.83	40.82	63.81	86.89	64.88	41.41	64.39	2.14	

TABLE II

AVERAGE DICE SCORES WHEN ALIGNING TO MODALITY T2 WHICH IS NOT IDEAL.

Method	T1				T2				T1ce				Flair								
	WT	TC	EC	Avg.	WT	TC	EC	Avg.	WT	TC	EC	Avg.	WT	TC	EC	Avg.	WT	TC	EC	Avg.	
Unimodal	72.96	65.59	37.77	58.77	82.65	66.76	45.23	64.91	71.41	73.30	76.36	73.69	81.91	63.57	40.74	62.07	84.31	67.59	43.17	65.02	65.90
KD-Net	72.09	65.37	40.83	59.43	60.02	80.78	67.64	45.59	64.67	66.22	73.61	78.86	78.72	77.07	77.98	84.31	67.59	43.17	65.02	65.90	64.71
PMKL	71.23	61.40	40.98	57.87	61.10	81.47	69.08	44.60	65.05	65.94	71.92	76.22	77.71	75.29	77.86	84.00	65.18	42.53	63.90	64.71	64.47
ProtoKD	72.95	67.37	40.73	60.35	61.91	83.85	68.51	45.70	66.02	66.28	75.08	79.93	78.50	77.84	77.46	84.36	68.16	41.48	64.46	64.47	64.47
SMU-Net	86.31	67.62	40.17	64.70	61.37	72.72	66.48	43.97	61.06	66.48	75.78	79.26	72.55	75.86	76.66	83.99	70.60	41.82	65.47	65.47	63.81

TABLE III

COMPARISON OF DICE SCORES WHEN DIFFERENT MODALITIES ARE MISSING. ● IS THE MODALITY WHICH IS NOT MISSING, ○ IS THE MODALITY WHICH IS MISSING. Δ IS THE MODEL WITH OUR PARADIGM.

Type	Flair	T1	T1ce	T2	WT	TC	EC	Avg.	WT	TC	EC	Avg.	WT	TC	EC	Avg.	WT	TC	EC	Avg.	
	○	○	○	●	○	○	●	○	●	●	●	●	●	●	●	○	●	●	●	●	Avg.
WT	PMKL	81.00	70.50	73.31	84.11	75.82	66.62	79.85	79.35	83.01	75.67	73.86	84.78	83.19	70.57	85.62	86.81	82.15	85.62	77.82	81.85
	Δ	83.77	75.97	72.04	85.70	77.98	74.34	83.82	83.00	85.09	83.85	81.86	85.27	86.13	82.15	86.81	82.15	82.15	86.81	82.15	81.85
TC	PMKL	67.92	76.92	64.26	62.21	72.46	70.05	51.64	66.66	68.74	66.44	70.12	61.79	75.04	68.89	80.14	68.22	79.22	71.47	71.47	71.47
	Δ	69.91	80.35	68.39	68.44	75.06	76.04	54.62	67.49	67.96	67.66	76.55	65.49	76.70	78.21	79.22	71.47	71.47	71.47	71.47	71.47
ET	PMKL	47.09	75.54	41.37	41.35	70.25	69.31	21.92	47.10	44.13	62.43	68.24	39.90	69.28	65.37	75.01	55.89	77.85	77.85	77.85	60.60
	Δ	45.17	76.44	47.66	43.57	73.37	77.88	36.78	46.00	45.24	61.90	78.79	44.86	75.47	77.96	77.85	55.89	77.85	77.85	77.85	60.60

between Z_j^* and these P_{mix} 's is tractable, and the feature and its target for alignment are paired. Therefore, we can exploit MSE as the alignment loss. However, P_{mix}^N utilizes the standard Gaussian distribution, not derived from a weighted combination of $\{P(Z_j^*)\}_1^J$, its relationship with $P(Z_j^*)$ is unclear. As such, the definitive alignment target for each feature remains unknown. Consequently, we can only use the KL divergence to align the entire distribution of $P(Z_j^*)$ to P_{mix}^N . Similar to VAE, given J modalities, our objective is to minimize $\mathbb{E}[D_{KL}(P(Z_j^*)||P_{mix}^N)]$, which is equivalent to minimizing: $\mathbb{E}[2 \log 1/v(Z_j^*) + v(Z_j^*)^2 + (\bar{Z}_j^*)^2/2 - 1/2]$, which was proposed in VAE. Here $v(Z_j^*)$, \bar{Z}_j^* denotes the variance and mean of Z_j^* , which are obtained by learnable parameters during the training process.

IV. EXPERIMENTS

Data and implementation details. The 2018 Brain Tumor Segmentation Challenge (BRATS) dataset [4], [20], consisting of 285 subjects with four MRI modalities (T1, T1c, T2, and FLAIR), is employed to evaluate the proposed paradigm and other baselines. Annotations are given by normal tissue regions and three tumor-related masks, i.e., whole tumor (WT), tumor core (TC), and enhancing core (EC). Image intensities are normalized to $[-1, 1]$. Each volume is augmented by randomly cropping each training example as $80 \times 80 \times 80$ [1], while the dataset is split following [13]. *Teachers* and *students* are optimized with Adam. Batch size is set as 4. Learning rates are initialized as $1e^{-3}$ which are gradually decayed by $1e^{-5}$ for both *teachers* and *students*.

TABLE IV
COMPARISON RESULTS OF *teacher* WITH DIFFERENT TYPES OF P_{mix} .
BEST RESULTS ARE HIGHLIGHTED IN **BOLD**.

P_{mix}	WT	TC	EC	Average
Without P_{mix}	85.62	80.14	75.01	80.26
P_{mix}^N	84.14	77.44	74.82	79.13
P_{mix}^k	86.34	79.75	76.91	81.00
P_{mix}^*	86.81	79.22	77.85	81.29

TABLE V
COMPARISON RESULTS OF *teachers* ON DIFFERENT SINGLE- MODALITY.
COLUMNS REPRESENT TARGET MODALITIES.

Modality	T1	T2	T1ce	Flair	Average
T1	58.92	55.27	9.89	22.15	36.56
T2	4.29	65.01	11.87	34.20	28.84
T1ce	38.19	11.70	76.76	37.95	41.15
Flair	5.05	40.47	40.17	62.14	36.96

A. Comparison with state-of-the-art methods

Table I reports how our proposal could promote state-of-the-art (SOTA) approaches in guiding *students*, including KD-Net [12], PMKL [1], ProtoKD [13] and SMU-Net [11]. When three modalities (the most challenging setting) are missing, the anchor P_{mix}^* could lead to an improvement of 1.75 dice score on average for various SOTA *students*. We also carry out experiments on other less difficult scenarios. These additional results can be referred to in Table III.

B. Find the teacher with the best prior knowledge

Figure 1 presents distributions of anchors among P_{mix}^N , P_{mix}^k , and P_{mix}^* . Consistent with the theoretical analysis presented in Sec. II, modality gaps are not narrowed at all. As such, the space cannot be filled with P_{mix}^N in (c), suggesting that $P_{mix}^N \triangleq \mathcal{N}(0, 1)$ cannot be placed as a fixed anchor to be aligned to. On the contrary, as shown in (d) and (e) when anchors P_{mix}^k and P_{mix}^* are employed, distributed centers of each modality are almost overlapped, demonstrating that modality gaps are narrowed. Table IV statistically demonstrates that P_{mix}^* , as the best anchor for *teacher*, generates an improvement by 1.03 dice score.

C. Effectiveness verification of the student

Proper P_{mix}^k to be aligned. To design a pre-defined anchor P_{mix}^k , we train the *teachers* with each single modality. As shown in Table V, treating T1ce modality as P_{mix}^k achieves the best dice score 41.15 across all the testing sets. This implies that T1ce encompasses the most comprehensive information, making it an ideal fixed anchor for enhancing feature invariant representation learning. Additionally, we also find that the learning parameters in P_{mix}^* of T1, T2, T1ce and Flair are 0.7759, 0.8977, 2.2055 and 0.3055 respectively. Apparently, T1ce enjoys the biggest weight, meaning that it is the most informative modality. Conversely, an unsuitable fixed anchor will significantly impair segmentation performance, as discussed in Table II.

Options of anchors. Table I also shows that *students* trained by *teachers* with P_{mix}^* performs better than *teachers* with P_{mix}^k ; in addition, *teachers* with P_{mix}^N is the worst one. P_{mix}^*

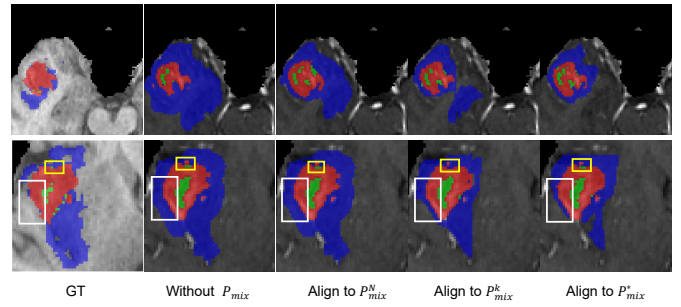


Fig. 2. Segmentation visualization on BraTS2018 [4], [20].

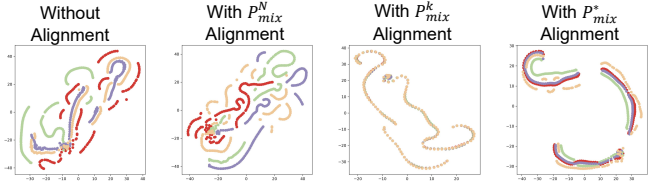


Fig. 3. Latent space feature visualization of *teachers* with different anchor P_{mix}^s for a specific sample. Different colors represent different modalities. Latent spaces aligned to P_{mix}^N and without alignment have obvious modality gaps, while latent spaces aligned to P_{mix}^k and P_{mix}^* have narrow gaps.

brings an improvement on *students* by 1.75 dice score on average while P_{mix}^k brings 1.28. Visualized demonstrations of aligning the latent representations to different anchors are displayed in Figure 2. In Figure 3, visualization results of the latent space for a specific sample are also shown. As observed, *teachers* with P_{mix}^N and P_{mix}^* are more sensitive to small targets (yellow boxes). Moreover, *teachers* with P_{mix}^k and P_{mix}^* are more likely to produce less false detection (white boxes). Overall, we can conclude that P_{mix}^* is indeed one effective anchor.

V. CONCLUSION

In this paper, we present a novel alignment framework to narrow the modality gaps whilst learning simultaneously invariant feature representations in segmenting brain tumors with missing modalities. Specifically, we invent an alignment paradigm for the *teacher* with latent space distribution P_{mix}^* as the aligning anchor, thereby building the reliable prior knowledge to supervise training *students*. Meanwhile, we provide theoretical support for the proposed alignment paradigm, demonstrating that individually aligning each modality to P_{mix}^* certifies a tighter evidence lower bound than mapping all modalities as a whole. Extensive experiments have demonstrated the superiority of the proposed paradigm in several latest state-of-the-art approaches, enabling them to better transfer knowledge from the multi-modality *teacher* to the *student* with missing modalities.

REFERENCES

- [1] C. Chen, Q. Dou, Y. Jin, Q. Liu, and P. A. Heng, "Learning with privileged multimodal knowledge for unimodal segmentation," *IEEE transactions on medical imaging*, vol. 41, no. 3, pp. 621–632, 2021.
- [2] Z. Zhao, H. Yang, and J. Sun, "Modality-adaptive feature interaction for brain tumor segmentation with missing modalities," in *International Conference on Medical Image Computing and Computer-Assisted Intervention*. Springer, 2022, pp. 183–192.
- [3] T. Lindig, R. Kotikalapudi, D. Schweikardt, P. Martin, F. Bender, U. Klose, U. Ernemann, N. K. Focke, and B. Bender, "Evaluation of multimodal segmentation based on 3d t1-, t2-and flair-weighted images—the difficulty of choosing," *Neuroimage*, vol. 170, pp. 210–221, 2018.
- [4] B. H. Menze, A. Jakab, S. Bauer, J. Kalpathy-Cramer, K. Farahani, J. Kirby, Y. Burren, N. Porz, J. Slotboom, R. Wiest *et al.*, "The multimodal brain tumor image segmentation benchmark (brats)," *IEEE transactions on medical imaging*, vol. 34, no. 10, pp. 1993–2004, 2014.
- [5] D. D. Patil and S. G. Deore, "Medical image segmentation: a review," *International Journal of Computer Science and Mobile Computing*, vol. 2, no. 1, pp. 22–27, 2013.
- [6] O. Maier, B. H. Menze, J. Von der Gabelentz, L. Häni, M. P. Heinrich, M. Liebrand, S. Winzeck, A. Basit, P. Bentley, L. Chen *et al.*, "Isles 2015—a public evaluation benchmark for ischemic stroke lesion segmentation from multispectral mri," *Medical image analysis*, vol. 35, pp. 250–269, 2017.
- [7] D. Chen, Y. Qiu, and Z. Wang, "Query re-training for modality-agnostic incomplete multi-modal brain tumor segmentation," in *International Conference on Medical Image Computing and Computer-Assisted Intervention*. Springer, 2023, pp. 135–146.
- [8] Y. Qiu, D. Chen, H. Yao, Y. Xu, and Z. Wang, "Scratch each other's back: Incomplete multi-modal brain tumor segmentation via category aware group self-support learning," in *Proceedings of the IEEE/CVF International Conference on Computer Vision*, 2023, pp. 21 317–21 326.
- [9] Y. Qiu, Z. Zhao, H. Yao, D. Chen, and Z. Wang, "Modal-aware visual prompting for incomplete multi-modal brain tumor segmentation," in *Proceedings of the 31st ACM International Conference on Multimedia*, 2023, pp. 3228–3239.
- [10] Y. Liu, L. Fan, C. Zhang, T. Zhou, Z. Xiao, L. Geng, and D. Shen, "Incomplete multi-modal representation learning for alzheimer's disease diagnosis," *Medical Image Analysis*, vol. 69, p. 101953, 2021.
- [11] R. Azad, N. Khosravi, and D. Merhof, "Smu-net: Style matching u-net for brain tumor segmentation with missing modalities," in *International Conference on Medical Imaging with Deep Learning*. PMLR, 2022, pp. 48–62.
- [12] M. Hu, M. Maillard, Y. Zhang, T. Ciceri, G. La Barbera, I. Bloch, and P. Gori, "Knowledge distillation from multi-modal to mono-modal segmentation networks," in *Medical Image Computing and Computer Assisted Intervention—MICCAI 2020: 23rd International Conference, Lima, Peru, October 4–8, 2020, Proceedings, Part I 23*. Springer, 2020, pp. 772–781.
- [13] S. Wang, Z. Yan, D. Zhang, H. Wei, Z. Li, and R. Li, "Prototype knowledge distillation for medical segmentation with missing modality," in *ICASSP 2023-2023 IEEE International Conference on Acoustics, Speech and Signal Processing (ICASSP)*. IEEE, 2023, pp. 1–5.
- [14] Y. Ganin, E. Ustinova, H. Ajakan, P. Germain, H. Larochelle, F. Laviolette, M. Marchand, and V. Lempitsky, "Domain-adversarial training of neural networks," *The journal of machine learning research*, vol. 17, no. 1, pp. 2096–2030, 2016.
- [15] S. Hu, K. Zhang, Z. Chen, and L. Chan, "Domain generalization via multidomain discriminant analysis," in *Uncertainty in Artificial Intelligence*. PMLR, 2020, pp. 292–302.
- [16] Y. Li, X. Tian, M. Gong, Y. Liu, T. Liu, K. Zhang, and D. Tao, "Deep domain generalization via conditional invariant adversarial networks," in *Proceedings of the European conference on computer vision (ECCV)*, 2018, pp. 624–639.
- [17] J. Tomczak and M. Welling, "Vae with a vampprior," in *International Conference on Artificial Intelligence and Statistics*. PMLR, 2018, pp. 1214–1223.
- [18] M. Havaei, N. Guizard, N. Chapados, and Y. Bengio, "Hemis: Hetero-modal image segmentation," in *Medical Image Computing and Computer-Assisted Intervention—MICCAI 2016: 19th International Conference, Athens, Greece, October 17–21, 2016, Proceedings, Part II 19*. Springer, 2016, pp. 469–477.
- [19] L. van der Maaten and G. Hinton, "Visualizing data using t-sne," *Journal of Machine Learning Research*, vol. 9, no. 86, pp. 2579–2605, 2008. [Online]. Available: <http://jmlr.org/papers/v9/vandermaaten08a.html>
- [20] S. Bakas, H. Akbari, A. Sotiras, M. Bilello, M. Rozycki, J. S. Kirby, J. B. Freymann, K. Farahani, and C. Davatzikos, "Advancing the cancer genome atlas glioma mri collections with expert segmentation labels and radiomic features," *Scientific data*, vol. 4, no. 1, pp. 1–13, 2017.